

CN-Cycle Solar Neutrinos and Sun's Primordial Core Metallicity

W. C. Haxton

*Institute for Nuclear Theory and Dept. Physics, University of Washington, Seattle, WA 98195,
USA*

`haxton@u.washington.edu`

and

A. M. Serenelli

Institute for Advanced Study, Princeton, NJ 08540, USA

`aldos@ias.edu`

ABSTRACT

We argue that it may be possible to exploit neutrinos from the CN cycle and pp chain to determine the primordial solar core abundances of C and N at an interesting level of precision. Such a measurement would allow a comparison of the Sun's deep interior composition with its surface, testing a key assumption of the standard solar model (SSM), a homogeneous zero-age Sun. It would also provide a cross-check on recent photospheric abundance determinations that have altered the once excellent agreement between the SSM and helioseismology. As further motivation, we discuss a speculative possibility in which photospheric abundance/helioseismology puzzle is connected with the solar-system metal differentiation that accompanied formation of the gaseous giant planets.

The theoretical relationship between core C and N and the ^{13}N and ^{15}O solar neutrino fluxes can be made more precise (and more general) by making use of the Super-Kamiokande and SNO ^8B neutrino capture rates, which calibrate the temperature of the solar core. The primordial C and N abundances can then be obtained from these neutrino fluxes and from a product of nuclear rates, with little residual solar model dependence. We describe some of the recent experimental advances that could allow this comparison to be made (theoretically) at the $\sim 9\%$ level, and note that this uncertainty may be reduced further due to ongoing work on the S-factor for $^{14}\text{N}(p,\gamma)$. The envisioned measurement might be possible in deep, large-volume detectors using organic scintillator, e.g., Borexino or SNO+.

Subject headings:

1. Introduction

Over three decades one of the most intriguing problems in physics and astrophysics has been that of the missing solar neutrinos, the discrepancy between Ray Davis’s chlorine-detector measurements (Davis et al. 1968; Bahcall & Davis 1976) and the predictions of the standard solar model (SSM) developed by Bahcall and collaborators (Bahcall et al. 2001; Bahcall & Pinsonneault 2004; Bahcall et al. 2006), by Turck-Chieze and collaborators (Brun et al. 1998, 1999), and others. Part of the problem’s fascination has been the tension between stellar theory and particle physics: arguments for new neutrino physics required one to believe that *ab initio* models correctly predicted the solar core temperature to an accuracy of about 1%.

Gradually the combination of quantitative tests of the solar model, particularly determinations of the interior sound speed via helioseismology, and new solar neutrino experiments, Kamioka (Fukuda et al. 1996), SAGE (Abdurashitov et al. 2003) and GALLEX/GNO (Kirsten 2003), and Super-Kamiokande (Fukuda et al. 2001, 2002), made the arguments for new physics compelling. The pattern of solar neutrino fluxes proved difficult to attribute to any plausible variation in the SSM. With the direct detection of both electron- and heavy-flavor solar neutrinos in the Sudbury Neutrino Observatory, solar neutrino experiments had not only demonstrated that electron neutrinos oscillate on their way to the earth, but also determined the parameters governing that oscillation (Ahmad et al. 2001, 2002a,b). Progress has continued with the KamLAND (Araki et al. 2005) reactor experiment and the Borexino collaboration’s efforts (Arpesella et al. 2008) to measure low-energy solar neutrinos in real time. Borexino’s recent results for the ${}^7\text{Be}$ solar neutrino flux are consistent with Large Mixing Angle (LMA) solution.

Because the incorporation of neutrino mass and mixing into the standard model requires new physics, the field’s attention has naturally turned to the unresolved particle physics questions, such as the mass hierarchy, mass scale, third mixing angle, and CP-violating phases. Mohapatra et al. (2004) summarizes the open questions and the envisioned future experimental program.

Here we return to one of the initial motivations for solar neutrino physics, using the neutrino flux as a probe of the SSM. We will argue that important tests of the Sun and its initial conditions can be made by measuring the CN-cycle neutrinos. Such a measurement would test a key assumption of the SSM – that convective mixing during the early pre-main-sequence Hayashi phase produced a homogeneous Sun, and that subsequent evolution has not appreciably altered the distribution of metals – an assumption that may now be in some degree of conflict with helioseismology. This assumption is the basis for taking the SSM’s primordial core metal abundances from today’s surface metal abundances. We argue that a series of recent advances – SNO and Super-Kamiokande measurements of the ${}^8\text{B}$ neutrinos, new cross section measurements for ${}^{14}\text{N}(p,\gamma)$ and for certain pp-chain reactions, and detector developments such as Borexino and SNO+, might allow one to determine the primordial abundances of C and N, with little dependence on the solar model: to good accuracy, these abundances can be derived from experimental quantities, namely the CN-cycle neutrino fluxes, the ${}^8\text{B}$ neutrino flux, and nuclear cross sections and oscillation parameters

measured in the laboratory.

Such a check of the SSM is of added interest because recent 3D modeling of photospheric absorption lines has led to a downward revision in the metal content of the solar convective zone (Asplund et al. 2005). This significantly alters the once spectacular agreement between the SSM and helioseismology in the temperature region below the solar convective zone, $\sim 2\text{-}5 \times 10^6$ K (Bahcall et al. 2005a,b; Antia & Basu 2005; Montalbán et al. 2004). In this region C, N, O, Ne, and Ar are partially ionized and particularly O and Ne have a significant influence on the radiative opacity.

A quantitative comparison between the Sun’s surface and core metallicities could prove useful in understanding the chemical evolution of other gaseous bodies in our solar system, whose interiors are not as easily probed. The Galileo and Cassini missions found significant metal enrichments in the H/He atmospheres of Jupiter and Saturn, e.g., abundances of C and N of \sim four times solar for Jupiter and \sim 4-8 for Saturn (Guillot 2005). Planetary models that take account of these data indicate that the gaseous giants are very significant solar-system metal reservoirs. We discuss, because of the size of these reservoirs and the time they were created, the possibility that they might have some connection with the current conflict between solar interior (helioseismology) and surface (photospheric absorption line) abundance determinations.

Finally, just as the solar neutrino program to date has provided our first quantitative test of the nuclear astrophysics governing proton burning in low-mass main-sequence stars, a solar CN-cycle neutrino program would give us our first experimental constraints on the process by which massive main-sequence stars burn hydrogen. The CN cycle is thought to have driven an early convective stage in our Sun, and is also important to the evolution of the first generation of massive metal-poor stars, where it turns on only after carbon has been synthesized by the triple alpha process.

2. The CNO Bi-Cycle and its Neutrinos

The need for two mechanisms to burn hydrogen was recognized in the pioneering work of Bethe and collaborators. The pp-chain, which dominates energy production in our Sun and other low-mass main-sequence stars, can be considered a primary process in which the chain’s “catalysts” – deuterium, ^3He , and $^7\text{Be}/^7\text{Li}$, the elements participating in intermediate steps shown in Fig. 1 – are synthesized as the chain burns to equilibrium.

But the sharper T -dependence of the CNO cycle is necessary to account for the structure of massive main-sequence stars. Unlike the pp-chain, the CNO bi-cycle (Fig. 2) is a secondary process: the catalysts for H burning are the pre-existing metals. Thus the CNO contribution to energy generation is directly proportional to the stellar-core number abundance of the primordial metals. The CN-cycle, denoted by I in Fig. 2, is an important SSM neutrino source. The cycle conserves the number abundance, but alters the distribution of metals as it burns into equilibrium, eventually achieving equilibrium abundances proportional to the inverse of the respective rates.

The reactions controlling early conversion of metals in the solar core and the approach to equilibrium are $^{12}\text{C}(p,\gamma)$ and $^{14}\text{N}(p,\gamma)$: these are the next-to-slowest and slowest rates in the lower-temperature CN cycle, respectively. The central temperature of the solar core at the onset of nuclear burning, $T_7 \sim 1.34$, corresponds to a ^{12}C lifetime of about $2 \cdot 10^7$ y. Thus the initial out-of-equilibrium CN-cycle conversion of ^{12}C to ^{14}N in the central region of the early Sun is complete and rapid. The associated energy release is thought to render the central portion of the solar core convectively unstable for a period of about 10^8 y. That is, the steep temperature dependence of $^{12}\text{C}(p,\gamma)$ produces composition, opacity, and thus thermal gradients sufficient to drive convection. The temperature at which the ^{12}C lifetime is comparable to the Sun’s 4.57 b.y. lifetime is $T_7 \sim 1.0$. In the SSM this includes essentially the entire energy-producing core, $R \lesssim 0.18R_\odot$ and $M \lesssim 0.29M_\odot$, so that nearly all of the core’s primordial ^{12}C has been converted to ^{14}N . This change in the chemical composition alters the opacity and, at the 3% level, the heavy-element mass fraction Z , SSM effects first explored by Bahcall & Ulrich (1988).

The $^{14}\text{N}(p,\gamma)$ reaction determines whether equilibrium has been achieved. The ^{14}N lifetime is shorter than the age of the Sun for $T_7 \gtrsim 1.33$. Therefore equilibrium for the CN cycle has been reached only for $R \lesssim 0.1R_\odot$, corresponding to the central 7% of the Sun by mass. Consequently, over a significant portion of the outer core, ^{12}C has been converted to ^{14}N , but further reactions are inhibited by the $^{14}\text{N}(p,\gamma)$ bottleneck.

The BSP08(GS) SSM (Peña-Garay & Serenelli 2008) – which employs values for Z and the $^{14}\text{N}(p,\gamma)$ S-factor given below – predicts a modest CN-cycle contribution to solar energy generation of 0.8% but substantial fluxes of neutrinos

$$\begin{aligned} ^{13}\text{N}(\beta^+)^{13}\text{C} \quad E_\nu &\lesssim 1.199 \text{ MeV} \quad \phi = (2.93_{-0.82}^{+0.91}) \times 10^8 / \text{cm}^2\text{s} \\ ^{15}\text{O}(\beta^+)^{15}\text{N} \quad E_\nu &\lesssim 1.732 \text{ MeV} \quad \phi = (2.20_{-0.63}^{+0.73}) \times 10^8 / \text{cm}^2\text{s}. \end{aligned}$$

Here uncertainties reflect conservative abundance uncertainties as defined empirically in Bahcall & Serenelli (2005). The first reaction is part of the path from ^{12}C to ^{14}N , while the latter follows $^{14}\text{N}(p,\gamma)$. Thus neutrinos from ^{15}O β decay are produced in the central core: 95% of the flux comes from the CN-equilibrium region, described above. About 30% of the ^{13}N neutrinos come from outside this region, primarily because of the continued burning of primordial ^{12}C : this accounts for the somewhat higher flux of these neutrinos. There is also a small but fascinating contribution from ^{17}F β decay,

$$^{17}\text{F}(\beta^+)^{17}\text{O} \quad E_\nu \lesssim 1.740 \text{ MeV} \quad \phi = (5.82 \pm 3.04) \times 10^6 / \text{cm}^2\text{s}$$

a reaction fed by (p,γ) on primordial ^{16}O : the cycling time for the second branch of the CNO bi-cycle, for solar core conditions, is much longer than the solar age. The flux of these neutrinos appears too small to allow a test of the Sun’s primordial oxygen content by this means (Bahcall 1989).

The SSM makes several reasonable assumptions, including local hydrostatic equilibrium (the balancing of the gravitational force against the gas pressure gradient), energy generation by pro-

ton burning, a homogeneous zero-age Sun, and boundary conditions imposed by the known mass, radius, and luminosity of the present Sun. It assumes no significant mass loss or accretion. The homogeneity assumption allows the primordial core metallicity to be fixed to today’s surface abundances. Corrections for the effects of diffusion of He and the heavy elements over 4.57 b.y. of solar evolution are included, and generally been helpful in improving the agreement between SSM predictions and parameters probed in helioseismology.

The assumption of a homogeneous zero-age Sun is based on arguments that the early pre-main-sequence Sun passed through a fully convective, highly luminous Hayashi phase, homogenizing the Sun. Yet, as recently discussed in Winnick et al. (2002), whether this homogeneity persists until the main sequence depends on the Sun’s metal accretion history. In the subsequent late pre-main-sequence phase (the Henyey phase), the Sun approaches the main sequence by establishing and growing a radiative core. Metals accreted onto the Sun in or after this phase would not be mixed into the core. Thus in principle, if the accreted material had a metal content that is not uniform in time, differences between the surface and core could arise in the Henyey phase. Winnick et al. (2002) have discussed scenarios in which such accretion might produce a convective zone enriched in metals relative to the radiative zone. For many years one motivation for models with such “low Z ” cores was to lower the ^8B neutrino flux, reducing the discrepancy between the SSM and the results of the Davis experiment.

The SSM assumes no such differentiation occurs. While this assumption of a homogeneous zero-age Sun may be correct, there are few observational checks on proto-solar evolution. But one possibility might be the CN-cycle neutrinos. The flux of these neutrino should depend nearly linearly on the initial core abundance of C and N. If other uncertainties affecting predictions of these fluxes could be brought under control, and if these fluxes were measured, constraints on the core’s primordial C and N might be obtained.

Solar surface abundances are known, determined from analyses of photospheric atomic and molecular spectral lines. Traditionally the associated solar atmosphere modeling has been done in one dimension, in a time-independent hydrostatic analysis that incorporates convection via mixing-length theory. But much improved 3D models of the solar atmosphere have been developed recently to treat the radiation-hydrodynamics and time dependence of this problem. This approach is essentially parameter-free and has been shown to accurately reproduce average line profiles, improve the consistency between different line measurements (e.g., among the various sources of C and O lines), and bring the solar abundances into better accord with other stars in the solar neighborhood. The improved analysis, however, substantially lowers the solar metallicity from the previous standard, $Z=0.0169$ (Grevesse & Sauval 1998), to $Z=0.0122$ (Asplund et al. 2005), and thus alters SSM predictions. Hereafter we denote these as the GS and AGS abundances, respectively.

Solar models that use the GS solar composition, the most up to date of which is the BPS08(GS) (Peña-Garay & Serenelli 2008) but including also the BP00 (Bahcall et al. 2001), BP04 (Bahcall

& Pinsonneault 2004) and BS05(OP) (Bahcall et al. 2005b) models, are in excellent agreement with those deduced from helioseismology. But those computed with the revised abundance are in much poorer agreement, with discrepancies exceeding 1% in the region just below the convective zone ($R \sim 0.65 - 0.70R_{\odot}$). Associated properties of the SSM, such as the depth of the convective zone and the surface He abundance, are also now in conflict with helioseismology. As extensively discussed in Bahcall et al. (2006) discrepancies are significantly above measurement and solar model uncertainties.

The reduced core opacity also lowers the SSM prediction of the temperature-dependent ^8B neutrino flux by about 20%: the predicted ^8B flux using the GS abundances and Opacity Project (Badnell et al. 2005) opacities, model BPS08(GS) is $5.95 \times 10^6/\text{cm}^2\text{s}$, which drops to $4.72 \times 10^6/\text{cm}^2\text{s}$ when AGS abundances are used, model BPS08(AGS). These results can be compared to the ^8B neutrino flux deduced from the 391-day salt-phase SNO data set of 4.94 ± 0.21 (stat) $^{+0.38}_{-0.34} \times 10^6/\text{cm}^2\text{s}$ (Aharmim et al. 2005). The Super-Kamiokande combined unbinned (binned) analysis using the salt-phase SNO data finds a best-fit flux of 4.91 (4.86) $\times 10^6/\text{cm}^2$ (Hosaka et al. 2006). Thus the BPS08(GS) and BPS08(AGS) predictions are 1.2 and 0.95 times the experimental central values of the combined analysis. Both results are consistent with experiment, given current experimental (9.5%) and theoretical ($\sim 16\%$) uncertainties.

Finally, we describe a speculative scenario to illustrate why a direct measurement of solar core metallicity might be important to our understanding of solar system formation. If one were to attempt to construct a solar model that reproduces both a sound-speed profile consistent with helioseismology and the Asplund et al. (2005) photospheric abundances, that model would likely have a convective zone that is *depleted* in metals relative to the radiative core, not elevated as in the low-Z model familiar from the solar neutrino puzzle. It is possible to envision a scenario where this could happen – one that connects the chemistry of the Sun’s convective zone with that of the planets. First, there is clear evidence that solar-system metal differentiation occurred, associated with the formation of the metal-rich gaseous giants Jupiter, Saturn, Neptune, and Uranus. The gaseous atmospheres of Jupiter and Saturn are believed to have been formed by accretion onto relatively small ($\sim 10 M_{\oplus}$) rocky/icy cores, at a time when solar formation is nearly complete and the bulk of the gas in the nebular disk has dissipated. These atmospheres are established over ~ 1 -10 million years (Bodenheimer & Lin 2002). It is thus plausible that the gaseous planets were formed after the sun had developed a radiative core and an isolated convective zone. Second, the amount of chemical differentiation in the gaseous giants is suggestive: modelers estimate that Jupiter’s total metal content is between 8 and 39 M_{\oplus} , or $Z \sim 2.5$ -12.3%, while that of Saturn is between 13 and 28 M_{\oplus} , or $Z \sim 13.7$ -29.4% (Saumon & Guillot 2004). The excess metal contained in all four gaseous giants, ~ 40 -90 M_{\oplus} depending on modeling uncertainties (Guillot 2005), is comparable to the apparent deficit of metal in the convective zone ($\sim 50 M_{\oplus}$), were one to associate the GS abundances with the radiative zone (formed from primordial gas) and the AGS abundances with the convective zone. The late-forming gaseous envelopes of Jupiter and Saturn could account for up to 40 M_{\oplus} of this excess.

Thus it is possible that some mechanism operating in a chemically altered disk – perhaps proto-planets scouring out metal-rich dust grains that have settled to the disk midplane – might result both in metal enrichment of the gaseous giants and a reservoir of metal-depleted gas in the circum-planetary disk. Could some portion of that gas later be deposited on the Sun, reducing the effective Z of the convective zone? This question has been raised once before, by Castro et al. (2007), who then explored helioseismology in a two-zone model motivated by this possibility. While we are not advocating for such a scenario, simple estimates, including those above, do seem to support its plausibility. Numerical calculations indicate that the time scale for the Sun to accrete gas, influenced gravitationally by a Jupiter-mass body orbiting at a distance ~ 5 AU, is relatively short, on the order of $\sim 5 \times 10^5$ yr (Strom et al. 1993). It has also been noted, based on the needed planetesimal deposition rate and the tidal radius (~ 0.36 AU) of a fully grown Jupiter, that the planet would have perturbed the orbits of about $2500 M_{\oplus}$ of gas, or 35% of the mass of the Sun’s present convective envelope (Podolak et al. 1993). Thus at least some of the conditions necessary for convective-zone dilution appear to be satisfied.

Though it is beyond the scope of the present paper, it might be worthwhile to pursue this question further, assuming late-time accretion of metal-depleted gas (motivated by the gaseous giant metal reservoirs and their assumed time of formation). While the work by Castro et al. (2007) is a first step in this direction, if one takes the accretion scenario seriously, then (depending on the timing of accretion with respect to the development of the radiative/convective zone boundary) there should be a memory of the accretion in the modern sun’s upper radiative zone – a transition region between GS interior abundances and AGS surface abundances which depends on the volume and composition of the accreted material. Helioseismology would thus become a probe of the solar system’s late-stage accretion history. This history would be linked to solar development: in the standard Hayashi-track description of the proto-Sun, the scenario would only make sense if the planet atmospheres were formed in the Henyey phase or later. However, recent numerical simulations of cloud collapse and early solar evolution found that the convective envelope develops earlier, spans the outer third of the proto-Sun by radius, and resembles closely that of the modern Sun (Wuchterl & Klessen 2001). This would extend the window for dilution of the convective zone to earlier times. Finally, the scenario would predict chemical correlations between the planets and convective zone in our sun and, perhaps, in other solar-like planetary systems.

The various threads summarized above, plus additional considerations we discuss in this paper, provide strong motivation for experiments measuring CN-cycle neutrinos:

- A measurement of the CN neutrino flux would provide an independent test of solar metallicity, complementing photospheric determinations.
- This measurement would test the SSM postulate of a homogeneous zero-age Sun, one of the assumptions important to helioseismology, the ^8B neutrino flux, and other SSM predictions that depend on the metallicity of the Sun’s interior radiative zones.
- It would place constraints on metal accretion that might have occurred subsequent to the

Hayashi phase, as the pre-main-sequence convective solar core is established.

- The current solar neutrino program has helped to demonstrate experimentally that the nuclear astrophysics foundations of our standard theory of low-mass main-sequence stellar evolution are valid. Solar CN-cycle neutrinos provide our one opportunity to extend such tests to the nuclear physics governing heavier main-sequence stars.
- It is conceivable that a quantitative comparison of the Sun’s surface and interior metallicities might be important to more general problems of chemical differentiation during solar-system formation.

3. The Sun as a Calibrated Laboratory

Independent of questions about the Sun’s pre-main-sequence evolution, one recognizes that the Sun’s inner core would have been mixed at the onset of the main sequence due to the initial out-of-equilibrium burning of ^{12}C . It has been recognized for many years that a measurement of the CN-cycle solar neutrino flux would, in principle, determine the metallicity of this core zone, allowing a comparison with abundance determined from the solar atmosphere. But in the past several years new developments have occurred that now seem to suggest such a measurement could be practical. These include:

- Accurate calibrations of the solar core temperature by SNO and Super-Kamiokande;
- Tight constraints on the oscillation parameters and matter effects that will determine the flavor content of the CN and ^8B neutrino fluxes;
- Recent measurements of the controlling reaction of the CN cycle, $^{14}\text{N}(p,\gamma)$, that have significantly reduced the nuclear physics uncertainties affecting SSM predictions of CN-cycle fluxes; and
- New ideas for high-counting rate experiments that would be sensitive to CN-cycle neutrinos, and from which reliable terrestrial fluxes could be extracted.

Our analysis uses previous SSM work in which the logarithmic partial derivatives $\alpha(i, j)$ for each neutrino flux ϕ_i are evaluated for the SSM input parameters β_j ,

$$\alpha(i, j) \equiv \frac{\partial \ln [\phi_i / \phi_i(0)]}{\partial \ln [\beta_j / \beta_j(0)]} \quad (1)$$

where $\phi_i(0)$ and $\beta_j(0)$ denote the SSM best values. This information, in combination with the assigned uncertainties in the β_j , then provides an estimate of the uncertainty in the SSM prediction of ϕ_i . In particular, crucial to the current analysis is the work of Bahcall & Serenelli (2005), who

evaluated the dependence on the mass fractions (measured relative to hydrogen) of different heavy elements,

$$\beta_j = \frac{\text{mass fraction of element } j}{\text{mass fraction of hydrogen}} \equiv X_j \quad (2)$$

Having this information not as a function of the overall metallicity Z , but as a function of the individual abundances, allows us to separate the “environmental” effects of the metals in the solar core from the special role of primordial C and N as catalysts for the CN cycle. By environmental effects we mean the influence of the metals on the opacity and thus the ambient core temperature, which controls the rates of neutrino-producing reactions of both the pp-chain and CN cycle. Simply put, our strategy here is to use the temperature-dependent ^8B neutrino flux to calibrate the environmental effects of the metals and of other SSM parameters, thus isolating the special CN-cycle dependence on primordial C+N. We find this primordial abundance can be expressed, with very little residual solar model uncertainty, in terms of the measured ^8B neutrino flux and nuclear cross sections that have been determined in the laboratory. In fact, we argue that the resulting expression is likely more general than the SSM context from which it is derived.

The partial derivatives allow one to define the power-law dependencies of neutrino fluxes, relative to the SSM best-value prediction $\phi_i(0)$

$$\phi_i = \phi_i(0) \prod_{j=1}^N \left[\frac{\beta_j}{\beta_j(0)} \right]^{\alpha(i,j)} \quad (3)$$

where the product extends over N SSM input parameters. This expression can be used to evaluate how SSM flux predictions will vary, relative to $\phi_i(0)$, as the β_j are varied. Alternatively, the process can be inverted: a flux measurement could in principle be used to constrain an uncertain input parameter.

The baseline SSM calculation for our calculations is BPS08(AGS) (Peña-Garay & Serenelli 2008), which uses the recently determined AGS abundances for the volatile elements C, N, O, Ne, and Ar, rather than the previous GS standard composition. It should be noted that AGS includes a downward revision by 0.05 dex of the Si photospheric abundance compared to GS and, accordingly, a similar reduction in the meteoritic abundances. The partial derivatives needed in the present calculation are summarized in Tables 1 (solar model parameters and nuclear cross sections) and 2 (abundances).

The SSM estimate of uncertainties in the various solar neutrino fluxes ϕ_i can be obtained by folding the partial derivatives with the uncertainties in the underlying β_j . In particular, it is convenient to decompose Eq. 3 into its dependence on solar parameters, non-CN metals, nuclear S-factors, and the primordial C and N abundances,

$$\phi_i = \phi_i^{SSM} \times \left(\prod_{j \in \{\text{Solar}\}} \left[\frac{\beta_j}{\beta_j(0)} \right]^{\alpha(i,j)} \prod_{j \in \{\text{Metals} \neq \text{C,N}\}} \left[\frac{\beta_j}{\beta_j(0)} \right]^{\alpha(i,j)} \right)$$

$$\times \prod_{j \in \{\text{Nuclear}\}} \left[\frac{\beta_j}{\beta_j(0)} \right]^{\alpha(i,j)} \prod_{j \in \{\text{C,N}\}} \left[\frac{\beta_j}{\beta_j(0)} \right]^{\alpha(i,j)}. \quad (4)$$

The two terms within the brackets will be designated “environmental” uncertainties – SSM solar and abundance parameters that primarily influence neutrino flux predictions through changes they induce in the core temperature. These are, respectively, the uncertainties in the photon luminosity L_\odot , the mean radiative opacity, the solar age, and calculated He and metal diffusion; and the fractional abundances of O, Ne, Mg, Si, S, Ar, and Fe. The estimated 1σ fractional uncertainties for the solar parameters have been previously evaluated and are listed in Table 3.

The heavy elements abundances in BPS08(AGS) are taken from the meteoritic abundances where available (Mg, Si, S, and Fe) and otherwise from photospheric abundances (for the volatile elements C, N, O, Ne, Ar). As mentioned before, the assigned historical/conservative 1σ fractional uncertainties shown in Table 4 were defined empirically in Bahcall & Serenelli (2005) by

$$\frac{\Delta\beta_i}{\beta_i} = \left| \frac{\text{Abundance}_i^{\text{GS}} - \text{Abundance}_i^{\text{AGS}}}{(\text{Abundance}_i^{\text{GS}} + \text{Abundance}_i^{\text{AGS}})/2} \right|. \quad (5)$$

This definition generates the uncertainties shown in Table 4.

The next term contains the effects of nuclear cross section uncertainties on flux predictions. The β_j are the S-factors for p+p (S_{11}), $^3\text{He} + ^3\text{He}$ (S_{33}), $^3\text{He} + ^4\text{He}$ (S_{34}), p + ^7Be (S_{17}), e + ^7Be (S_{e7}), and p + ^{14}N (S_{114}). Their estimated 1σ fractional uncertainties, which we discuss below, are also shown in Table 3.

The last term is the contribution of the primordial C and N abundances. As Table 2 shows, pp-chain neutrino fluxes are relatively insensitive to variations in these abundances, as the heavier nuclei like Fe have a more important influence on the core opacity. But the expected, nearly linear response of the ^{13}N and ^{15}O neutrino fluxes to these abundances is apparent. These are the abundances we would like to constrain by a future measurement of the ^{13}N and ^{15}O solar neutrino fluxes. Such a measurement begins to be of interest if these abundances could be determined with an accuracy significantly better than 30%. Note that the C/N abundance term in Eq. (4) for $\phi(^{13}\text{N})$

$$\prod_{j \in \{\text{C,N}\}} \left[\frac{\beta_j}{\beta_j(0)} \right]^{\alpha(i,j)} = \left(\frac{X(^{12}\text{C})}{X(^{12}\text{C})_{SSM}} \right)^{0.874} \left(\frac{X(^{14}\text{N})}{X(^{14}\text{N})_{SSM}} \right)^{0.142} \quad (6)$$

is not quite linear in the overall C+N abundance. An overall scaling of primordial C and N, $X/X_{SSM} \rightarrow 1+\delta$ yields the dependence $(1+\delta)^{1.016}$, so 2% steeper than linear. In addition to the direct dependence of the CN-cycle on C and N, increasing the C+N abundance also increases the opacity and core temperature, to which the CN neutrino flux also responds.

Were one to vary the 11 SSM parameters designated as “environmental” according to their assigned uncertainties (taking them to be uncorrelated), an 7.5% SSM net uncertainty in $\phi(^{13}\text{N})$ would be obtained. But we can do better than this by exploiting SNO and Super-Kamiokande measurements of the ^8B neutrino flux, a “thermometer” that is even more sensitive to the solar core environment than the CN neutrinos. Below we discuss the use of SNO in this way – the arguments are simpler for this detector, because it provides a measurement of the ^8B neutrino flux independent of flavor. In the next section we use Super-Kamiokande, the case of most interest because it exploits the same reaction, elastic scattering, as the proposed CN-neutrino detectors, allowing some common errors to cancel: the SNO results then become crucial input, helping to constrain the effects of neutrino oscillations.

One can express $\phi(^{13}\text{N})$ uncertainties in terms of $\phi(^8\text{B})$, while minimizing the residual solar environmental error, i.e. by minimizing the contribution of the factor in parenthesis in the expression

$$\begin{aligned} \frac{\phi(^{13}\text{N})}{\phi^{SSM}(^{13}\text{N})} &= \left[\frac{\phi(^8\text{B})}{\phi^{SSM}(^8\text{B})} \right]^{K_{(13,8)}} \\ &\times \left(\prod_{j \in \{\text{Solar}\}} \left[\frac{\beta_j}{\beta_j(0)} \right]^{\gamma_j} \prod_{j \in \{\text{Metals} \neq \text{C,N}\}} \left[\frac{\beta_j}{\beta_j(0)} \right]^{\gamma_j} \right) \\ &\times \prod_{j \in \{\text{Nuclear}\}} \left[\frac{\beta_j}{\beta_j(0)} \right]^{\gamma_j} \prod_{j \in \{\text{C,N}\}} \left[\frac{\beta_j}{\beta_j(0)} \right]^{\gamma_j} \end{aligned} \quad (7)$$

where

$$\gamma_j \equiv \alpha(^{13}\text{N}, j) - K_{(13,8)} \alpha(^8\text{B}, j) \quad (8)$$

by a suitable choice of the constant $K_{(13,8)}$. Using the SSM logarithmic derivatives $\alpha(i, j)$ and parameter uncertainties $\Delta\beta_j/\beta_j$ of Tables 1-4, we find $K_{(13,8)} = 0.608$. To check the consistency of this procedure, we have performed a Monte Carlo simulation of solar models where the 11 environmental input quantities have been varied simultaneously. We find a tight correlation between the $\phi(^{13}\text{N})$ and $\phi(^8\text{B})$ fluxes. In Figure 3 we show this correlation on the top-left panel and the linear fit to the data, from which we find $K_{(13,8)} = 0.599$, the value we adopt for this paper, very close to that derived from the power-law exponents. The top-right panel shows the residuals of the fit and its standard deviation $\sigma = 2.8\%$. We note here that the bulk of the dispersion in the $\phi(^8\text{B}) - \phi(^{13}\text{N})$ correlation is due to the uncertainty in the diffusion rate. This can be understood as follows. All environmental quantities affect these neutrino fluxes by modifying the temperature in the solar core. Diffusion has, however, the additional effect of increasing the number of CN nuclei in the core, leading to a directly proportional increase in $\phi(^{13}\text{N})$ but not in $\phi(^8\text{B})$. This can be seen in Tables 1 and 2, where all the power-law exponents for environmental quantities are larger for $\phi(^8\text{B})$ than for $\phi(^{13}\text{N})$ (a natural consequence of the larger temperature dependence of $\phi(^8\text{B})$). The only exception is diffusion, on which $\phi(^{13}\text{N})$ shows a stronger dependence than $\phi(^8\text{B})$. Were we to exclude diffusion as a source of uncertainty, the dispersion in the $\phi(^8\text{B}) - \phi(^{13}\text{N})$ correlation would only be $\sim 0.5\%$.

Expressing $\phi(^{13}\text{N})$ in the form of Eq. (7) has two advantages. First, as we detail below, it reduces the overall theoretical uncertainty in the relationship between the primordial C and N abundances and the ^{13}N neutrino flux. Second, this relationship should be more general than the SSM context from which it is derived: the correlation between the various neutrino fluxes ϕ_i and T_c has been demonstrated to hold even when SSM parameters have been varied far outside their accepted SSM uncertainties.

A simple way to fix the first term on the right-hand side of Eq. (7) is by using the SNO measurement of the total ^8B neutrino flux, thereby eliminating many SSM and LMA oscillation parameter uncertainties in terms of a measured quantity. As the SNO statistical and systematic errors combined in quadrature give an uncertainty 9.4%, the net uncertainty in this term is then 5.6%. The remaining environmental uncertainty is encoded in the bracketed terms in Eq. (7), the deviations in the dependence of the ^{13}N and ^8B neutrino fluxes from a naive T_c power law. From our Monte Carlo simulation we find this residual uncertainty is 2.8%, and thus quite small in comparison to the SNO uncertainty: the total environmental uncertainty is $\sim 6.3\%$. The use of the SNO result to constrain the environmental uncertainty thus reduces this uncertainty, relative to the result obtain previously by direct variation of SSM input parameters within their assigned SSM uncertainties.

The remaining uncertainty arising in the evaluation of Eq. (7) is the nuclear factor which, given that the expression involves both the ^{14}N and ^8B fluxes, depends on a combination of pp-chain and CN-cycle S-factors. One finds from Tables 1- 4 that the uncertainties are dominated by S_{17} , S_{34} , which controls the pp-chain branching to the ppII and ppIII cycles, and S_{114} . One of the reasons that the CN neutrino fluxes are potentially a quantitative probe of the Sun’s primordial C and N are recent improvements particularly in determinations of the last two S-factors.

The traditional SSM value for S_{34} is based on the 1998 evaluation of Adelberger et al. (1998), 0.53 ± 0.05 keV b. The relatively large error bar on the recommended value reflected apparent systematic disagreements between experiments detecting prompt γ rays and counting the ^7Be activity. Since this evaluation new, high-statics measurements have been made by a Weizmann Institute group (Nara Singh et al. 2004, an activity measurement), by the LUNA collaboration (Confortola et al. 2007, a combination of prompt γ and activity measurements, as well as Gyürky et al. 2007, an activity measurement), and by the Seattle group (Brown et al. 2007, an activity measurement). If these data are extrapolated to threshold with the same theoretical fitting function, one finds values of $S(0)$ of 0.546 ± 0.020 , 0.560 ± 0.017 , 0.545 ± 0.017 , and 0.595 ± 0.018 keV b, respectively. The spread of these results is somewhat larger than is expected on the basis of the uncertainties. They have been combined by Snover (private communication) in a way that takes into account this spread by inflating the errors according to the associated chi-squares, while also accounting for possible correlations between the LUNA activity and total results (Gyürky et al. 2007; Confortola et al. 2007). The result is 0.564 ± 0.020 keV b. There is an additional theoretical uncertainty associated with the theoretical fitting function that is used to extrapolate these data to threshold to obtain $S(0)$. As discussed in Brown et al. (2007), generally this variation is at the few

percent level, though it can reach higher values if fits are required to reproduce higher-energy data. The procedure we followed is based on the LUNA group’s work on its activation data (Gyürky et al. 2007), where three theoretical models (Kajino & Arima 1984; Csótó & Langanke 2000 and Descouvemont et al. 2004) were used to derived an extrapolated zero-energy result. The resulting best values for $S(0)$ have a range of $\pm .019$ keV b, or $\pm 3.4\%$. Thus we adopt 3.4% as a theoretical extrapolation uncertainty, which we combine in quadrature with the Snover recommendation to obtain a final result of 0.564 ± 0.028 . This corresponds to a 4.9% uncertainty, which can be compared to the 9.4% uncertainty recommended in the Adelberger et al. (1998) evaluation.

The most important nuclear physics uncertainty in the analysis is $S(0)$ for $^{14}\text{N}(p,\gamma)$, a reaction that has been the subject of recent intense study. The S_{114} value and the 8.4% uncertainty adopted in Bahcall et al. (2006), 1.69 ± 0.14 keV b, was obtained from combining the LUNA results of Formicola et al. (2004), 1.7 ± 0.2 keV b (determined from data taken at or above center-of-mass energies of 140 keV), with the TUNL results of Runkle et al. (2005), 1.68 ± 0.09 (stat) ± 0.16 (sys) keV b. Subsequently a series of measurements have been done at LUNA in which the cross section was measured to center-of-mass energies as low as 70 keV (Imbriani et al. 2005; Lemut et al. 2006; Bemmerer et al. 2006; Trautvetter et al. 2008). In particular, Imbriani et al. (2005) give $S(0) = 1.61 \pm 0.08$ keV b, corresponding to a 5% error, based on data obtained for center-of-mass energies between 119 and 367 keV. We use the Imbriani value for $S(0)$ in this paper, a conservative choice given that this fit was made prior to the extension of measurements to 70 keV. Furthermore, work is underway on the energy range above the lowest resonance, ~ 300 -400 keV, a region which limits the interference pattern analysis, and on improved r-matrix analyses (Wiescher, private communication) which take into account all reaction channels. Thus we expect a more definite analysis of $S(0)$ and of its experimental and theoretical uncertainties will be available soon.

All of this can then be summarized in the theoretical relationship:

$$\begin{aligned} \frac{\phi(^{13}\text{N})}{\phi^{SSM}(^{13}\text{N})} &= \left[\frac{\phi^{SNO}(^8\text{B})}{\phi^{SSM}(^8\text{B})} \right]^{0.599} \\ &\times [1 \pm 2.8\%(\text{resid. environ.}) \pm 5.0\%(\text{nuclear})] \\ &\times \left(\frac{X(^{12}\text{C})}{X(^{12}\text{C})_{SSM}} \right)^{0.858} \left(\frac{X(^{14}\text{N})}{X(^{14}\text{N})_{SSM}} \right)^{0.141} . \end{aligned} \quad (9)$$

The first term, given the SNO total flux combined error of $\sim 9.4\%$, has an uncertainty of 6.4%. Thus one consequence of the recent work on pp-chain and CN-cycle S-factors is the reduction of the nuclear physics uncertainties to the level of the SNO measurements. The overall uncertainty, adding the SNO, residual environmental, and nuclear uncertainties in quadrature, is 8.6%, small compared to the conservative uncertainty assigned to the AGS abundances of $\sim 30\%$.

Under an overall scaling of primordial C and N, $X/X_{SSM} \rightarrow 1+\delta$, the quantity being constrained responds as

$$(1 + \delta)^{0.999} \sim 1 + \delta \quad (10)$$

Because we have removed the “environmental” effects of all metals in Eq. (9), we find the expected, nearly exact linear proportionality between the primordial metals C and N and the CN neutrino flux.

The arguments can be repeated for the ^{15}O flux, the more interesting case experimentally because of its higher endpoint energy. We find

$$\begin{aligned} \frac{\phi(^{15}\text{O})}{\phi^{SSM}(^{15}\text{O})} &= \left[\frac{\phi(^{8}\text{B})}{\phi^{SSM}(^{8}\text{B})} \right]^{0.828} \\ &\times \left(\prod_{j \in \{\text{Solar}\}} \left[\frac{\beta_j}{\beta_j(0)} \right]^{\gamma_j} \prod_{j \in \{\text{Metals} \neq \text{C,N}\}} \left[\frac{\beta_j}{\beta_j(0)} \right]^{\gamma_j} \right) \\ &\times \prod_{j \in \{\text{Nuclear}\}} \left[\frac{\beta_j}{\beta_j(0)} \right]^{\gamma_j} \prod_{j \in \{\text{C,N}\}} \left[\frac{\beta_j}{\beta_j(0)} \right]^{\gamma_j} \end{aligned} \quad (11)$$

where

$$\gamma_j \equiv \alpha(^{15}\text{O}, j) - 0.828\alpha(^{8}\text{B}, j). \quad (12)$$

The lower two panels in Figure 3 show the tight correlation between the $\phi(^{15}\text{O})$ and $\phi(^{8}\text{B})$ fluxes and the residuals of the linear fit.

Evaluating associated parameter uncertainties as before, one finds

$$\begin{aligned} \frac{\phi(^{15}\text{O})}{\phi^{SSM}(^{15}\text{O})} &= \left[\frac{\phi^{SNO}(^{8}\text{B})}{\phi^{SSM}(^{8}\text{B})} \right]^{0.828} \\ &\times [1 \pm 2.6\%(\text{resid. environ.}) \pm 7.1\%(\text{nuclear})] \\ &\times \left(\frac{X(^{12}\text{C})}{X(^{12}\text{C})_{SSM}} \right)^{0.805} \left(\frac{X(^{14}\text{N})}{X(^{14}\text{N})_{SSM}} \right)^{0.199} \end{aligned} \quad (13)$$

The larger environmental parameter, 0.828, is expected because the ^{15}O neutrino flux has a somewhat steeper dependence on the average core temperature than the ^{13}N flux. This increases the errors associated with SNO uncertainties (7.8%) and nuclear cross sections (the uncertainty in S_{34} and other pp-chain cross sections determines the quality of our ^{8}B neutrino thermometer). Thus the overall uncertainty in this “theoretical” relation between the ^{15}O neutrino flux and the core C/N abundance is 10.8%. As before, if one considers a scaling of primordial C and N, $X/X_{SSM} \rightarrow 1+\delta$, the last term becomes

$$(1 + \delta)^{1.004} \sim 1 + \delta \quad (14)$$

showing the linear relationship between the ^{15}O neutrino flux and the primordial C+N abundance.

Now we discuss a somewhat more detailed (and improved) analysis that exploits similarities between Super-Kamiokande and future CN neutrino detectors, and allows us to fold in what we have learned about neutrino oscillations from terrestrial experiments like KamLAND.

4. The Analysis for Elastic Scattering and Neutrino Oscillations

Equations (7) and (11) give relationships among the primordial core C and N abundances, other SSM uncertainties, and the instantaneously produced CN-cycle and ^8B neutrino fluxes. These equations, attractive because of their simplicity, are somewhat idealized, because they do not address how the left-hand sides of these equations will be determined experimentally. For example, neutrino oscillations during the transit to the earth will alter the flavors of these neutrino in an energy-dependent way, influencing detector responses. Fluxes determined in most experiments will have to be corrected for such effects, including the uncertainties in the neutrino mass difference δm_{12}^2 and mixing angle $\sin^2 2\theta_{12}$. In the discussion of the previous section, we avoided this issue in evaluating the right-hand sides of Eq. (7) and (11) by employing the SNO result for the total ^8B neutrino flux. But the first results on the CN-cycle fluxes, needed on the left-hand sides of Eqs. (7) and (11), are most likely to come from ν -e inelastic scattering experiments, where $\sigma(\nu_\mu)/\sigma(\nu_e) \sim 0.15$. Thus to derive the instantaneous (solar) values of these fluxes, one would have to correct the detector response for the effects of flavor mixing. Oscillations are one of several uncertainties that will produce correlated responses in both ^8B and CN neutrino detectors. Thus we need an analysis that accounts for such correlations: it is advantageous to develop this analysis, as one can then make use of another statistically powerful experiment (Super-Kamiokande) while supplementing SNO data with other constraints on flavor mixing (e.g., KamLAND).

Below we compare Super-Kamiokande and Borexino/SNO+ rates, which exploit a common detection mechanism, ν_x -e elastic scattering, making correlated errors easier to identify. Super-Kamiokande is potentially the best solar thermometer because of its statistical precision.

In this approach we express the total ^8B flux (the instantaneous solar flux needed in Eqs. (7) and (11)) as

$$\begin{aligned} \frac{\phi(^8\text{B})}{\phi^{SSM}(^8\text{B})} &= \frac{\phi(^8\text{B})\langle\sigma^{SK}(^8\text{B}, \delta m_{12}^2, \theta_{12})\rangle}{\phi^{SSM}(^8\text{B})\langle\sigma^{SK}(^8\text{B}, \delta m_{12}^2, \theta_{12})\rangle} \\ &\equiv \frac{R_{exp}^{SK}(^8\text{B})}{R_{cal}^{SK}(^8\text{B}, \delta m_{12}^2, \theta_{12})} \end{aligned} \quad (15)$$

Here $\langle\sigma^{SK}\rangle$ is an effective cross section that takes into account all of the neutrino flavor and detector response (trigger efficiencies, resolution, cross section uncertainties, etc.) issues that determine the relationship between a measured detector rate and the instantaneous solar flux. The numerator of the ratio on the right is a directly measured experimental quantity: the Super-Kamiokande elastic scattering rate for producing recoil electrons with apparent energies between 5.0 and 20 MeV, per target electron per second. The denominator is a conversion factor that relates the instantaneous ν_e flux to the experimental rate: the cross section for $\nu_x - e$ elastic scattering, averaged over a normalized ^8B spectrum, defined for the specific experimental conditions of Super-Kamiokande, and including the effects of flavor mixing. This conversion factor is essentially a laboratory quantity: it can be calculated from laboratory measurements of detector properties, the β decay spectrum, the underlying neutrino-electron cross sections, and most critically, the

parameters governing oscillations. We describe these factors below.

The experimental rate comes from the 1496 days of measurements of Super-Kamiokande I (Hosaka et al. 2006). From the SK I rate/kiloton/year

$$520.1 \pm 5.3(\text{stat}) \begin{matrix} +18.2 \\ -16.6 \end{matrix}(\text{sys}) \text{ kton}^{-1} \text{ y}^{-1}. \quad (16)$$

we find $R_{exp}^{SK}({}^8\text{B})$,

$$4.935 \pm 0.05(\text{stat}) \begin{matrix} +0.17 \\ -0.16 \end{matrix}(\text{sys}) \times 10^{-38} \text{ electron}^{-1}\text{s}^{-1} \quad (17)$$

(or ~ 0.049 Solar Neutrino Units, or SNU). The dominant systematic error includes estimates for the energy scale and resolution, trigger efficiency, reduction, spallation dead time, the gamma ray cut, vertex shift, background shape for signal reduction, angular resolution, and lifetime uncertainties. The combined statistical and systematic error is $\sim \pm 3.6\%$.

To evaluate the denominator in Eq. (15) we need the suitably averaged cross section, defined for the window used by the SK I collaboration,

$$\begin{aligned} \langle \sigma^{SK}({}^8\text{B}, \delta m_{12}^2, \theta_{12}) \rangle &= \int dE_\nu \phi_{norm}^{8\text{B}}(E_\nu) \\ &\times \left[P_{\nu_e}(E_\nu, \delta m_{12}^2, \sin^2 2\theta_{12}) \int_{T=0}^{T^{max}(E_\nu)} dT \sigma_{\nu_e}^{es}(T) \right. \\ &\left. + P_{\nu_\mu}(E_\nu, \delta m_{12}^2, \sin^2 2\theta_{12}) \int_{T=0}^{T^{max}(E_\nu)} dT \sigma_{\nu_\mu}^{es}(T) \right] \\ &\times \int_{5.0 \text{ MeV}}^{20.0 \text{ MeV}} d\epsilon_a f_{\text{trigger}}(\epsilon_a) \rho(\epsilon_a, \epsilon_t = T + m_e) \end{aligned} \quad (18)$$

where $\phi_{norm}^{8\text{B}}(E_\nu)$ is the normalized ${}^8\text{B}$ neutrino spectrum. Equation (18) involves an integral over the product of this spectrum and the energy-dependent oscillation probabilities. ($P_{\nu_e} + P_{\nu_\mu} = 1$, assuming oscillations into active flavors. P_{ν_μ} can be defined as the oscillation probability to heavy flavors, if the effects of three flavors are considered.) A given E_ν fixes the range of kinetic energies T of the scattered electron, over which an integration is done; in the laboratory frame $T^{max} = 2E_\nu^2/(m_e + 2E_\nu)$. The integrand includes the elastic scattering cross sections $\sigma^{es}(T)$ for electron and heavy-flavor neutrinos and the Super-Kamiokande resolution function $\rho(\epsilon_a, \epsilon_t)$, where $\epsilon_t = T + m_e$ is the true total electron energy while ϵ_a is apparent energy, as deduced from the number of phototube hits in the detector. Finally, an integral must be done over the window used by the experimentalists, apparent electron energies ϵ_a between 5.0 and 20.0 MeV. The deduced counting rate includes the triggering probability that a event of apparent energy ϵ_a will be recorded in the detector.

As the uncertainties associated with triggering efficiencies, energy scale, and resolution are already incorporated in the deduced Super-Kamiokande event rate (Eq. 16), we are free to use best-value functions in such an analysis. Here we employ simple fits to the measurements given in Hosaka et al. (2006), a Gaussian resolution function

$$\rho(\epsilon_a, \epsilon_t) = \frac{1}{\sqrt{2\pi}\sigma(\epsilon_t)} \exp \left[-\frac{(\epsilon_t - \epsilon_a)^2}{2\sigma(\epsilon_t)^2} \right] \quad (19)$$

where $\sigma(\epsilon_t) \sim 0.326\epsilon_t^{0.642}$, or about 14% at 10 MeV; and a relatively sharp trigger efficiency

$$f_{\text{trigger}}(\epsilon_a) = \frac{1}{2} + \frac{1}{2} \tanh^5 \left[\frac{\epsilon_a - \bar{\epsilon}_a}{\sigma'} \right] \quad (20)$$

where $\bar{\epsilon}_a \sim 3.6$ MeV and $\sigma' \sim 0.172$ MeV.

The expression for the CN-cycle neutrino response is similar to Eq. (15)

$$\begin{aligned} \frac{\phi(^{15}\text{O})}{\phi^{SSM}(^{15}\text{O})} &= \frac{R_{exp}^{B/S}(^{15}\text{O})}{\phi^{SSM}(^{15}\text{O}) \langle \sigma^{B/S}(^{15}\text{O}, \delta m_{12}^2, \theta_{12}) \rangle} \\ &\equiv \frac{R_{exp}^{B/S}(^{15}\text{O})}{R_{cal}^{B/S}(^{15}\text{O}, \delta m_{12}^2, \theta_{12})} \\ &= \frac{R_{exp}^{B/S}(\text{CN}) / (1 + \alpha(0.8, 1.3))}{R_{cal}^{B/S}(^{15}\text{O}, \delta m_{12}^2, \theta_{12})} \end{aligned} \quad (21)$$

Here the experimental rate for ^{15}O neutrinos has been written in terms of the total CN-neutrino rate $R_{exp}^{B/S}(\text{CN})$ by introducing a correction factor α discussed below. No measurement of $R_{exp}^{B/S}(\text{CN})$ currently exists, of course. But such measurements could be made in Borexino or SNO+, existing or planned detectors that will use large volumes of organic scintillator, placed quite deep underground (we discuss these detectors in the concluding section). A window for the apparent kinetic energy T of the scattered electron of 0.8-1.3 MeV has been discussed by the Borexino group. As the ^7Be 0.866 MeV line corresponds to $T^{max} \sim 0.668$ MeV, this window would limit contamination from ^7Be neutrino recoil electrons. As Borexino has achieved a resolution of $\sim 8.7\%$ at $T = 751$ MeV and $\sim 9.1\%$ at 0.825 MeV, we take (for simulation purposes) a Gaussian resolution function (Eq. 19) with

$$\sigma(T) \sim 0.08 \text{MeV} \sqrt{T/\text{MeV}} \quad (22)$$

We also adopt a nominal step-function trigger, $f_{\text{trigger}} = \theta(T - 0.25 \text{MeV})$, though the trigger does not influence rates in the high-energy window of interest for CN neutrinos.

The factor $\alpha(0.8, 1.3) \sim 0.120$ is the ratio of the measured ^{13}N to ^{15}O neutrino rates in the observation window, a correction we introduce to convert the total rate to the rate for ^{15}O neutrinos. In principle this is a measurable quantity: because of the lower endpoint, the relative importance of ^{13}N neutrinos drops quickly with energy. For the ^{15}O neutrinos, 60% of the events would reside in bins between 0.8-1.0 MeV, with the remaining 40% between 1.0-1.3 MeV. If one looks at total events (^{13}N and ^{15}O), ^{13}N neutrinos are responsible for $\sim 19\%$ of the events between 0.8-1.0 MeV, but only 1.0% of those between 1.0-1.3 MeV, taking BPS08(AGS) SSM best-value fluxes. Such a bin analysis will have to contend with the contribution from the line-source pep neutrinos as well, however, so the accuracy with which α can be measured is certainly not clear.

However, an experimental determination is probably not required. We can write α as

$$\alpha = \frac{\phi(^{13}\text{N}) \langle \sigma^{B/S}(^{13}\text{N}, \delta m_{12}^2, \theta_{12}) \rangle}{\phi(^{15}\text{O}) \langle \sigma^{B/S}(^{15}\text{O}, \delta m_{12}^2, \theta_{12}) \rangle} \quad (23)$$

The cross section ratio can be evaluated, yielding $0.086(1 \pm 0.0036)$, when the LMA oscillation parameters are varied over the full range allowed by the KamLAND combined analysis. The reason for the very small error is that variations in these parameters tend to affect the two cross sections identically: the 0.8-1.3 MeV event window is narrow, and clearly differences must vanish in the limit of a zero-width window. The flux ratio at the parameter point defined by the BPS08(AGS) SSM best values is 1.40. The changes in this ratio obtained by varying SSM parameters can be evaluated by procedures similar to those leading to Eqs. (9) and (13),

$$\begin{aligned} \alpha &= 0.120(1 \pm .0036) \left[\frac{\phi^{SNO}(^8\text{B})}{\phi^{SSM}(^8\text{B})} \right]^{-0.229} \\ &\times [1 \pm 0.24\%(\text{resid. envir.}) \pm 2.0\%(\text{nuclear})] \\ &\times \left(\frac{X(^{12}\text{C})}{X(^{12}\text{C})_{SSM}} \right)^{0.053} \left(\frac{X(^{14}\text{N})}{X(^{14}\text{N})_{SSM}} \right)^{-0.058} \end{aligned} \quad (24)$$

One finds that α is stable under reasonable parameter variations: changes induced by the nuclear physics or core temperature tend to affect these fluxes in similar ways. This includes variations in core metals, the quantity we hope to constrain: adjustments in the C or N primordial abundance by 30% produce changes at or below 1.5%, that is, $0.120 (1 \pm 0.015)$. If the overall metallicity is changed, keeping the C/N ratio fixed, this becomes 0.1%. One concludes from these exercises that the ratio of events in the 0.8-1.3 MeV window from ^{13}N and ^{15}O neutrino interactions to that from ^{15}O neutrinos alone, is 1.120 ± 0.003 , when all sources of uncertainty are considered.

The final step is to plug Eqs. 15 and 21 into Eq. 11 to obtain

$$\begin{aligned} \frac{R_{exp}^{B/S}(\text{CN})}{R_{cal}^{B/S}(^{15}\text{O}, \delta m_{12}^2, \theta_{12})} &= \\ (1.120 \pm 0.003) &\left[\frac{R_{exp}^{SK}(^8\text{B})}{R_{cal}^{SK}(^8\text{B}, \delta m_{12}^2, \theta_{12})} \right]^{0.828} \\ &\times [1 \pm 2.6\%(\text{resid. envir.}) \pm 7.6\%(\text{nuclear})] \\ &\times \left(\frac{X(^{12}\text{C})}{X(^{12}\text{C})_{SSM}} \right)^{0.805} \left(\frac{X(^{14}\text{N})}{X(^{14}\text{N})_{SSM}} \right)^{0.199} . \end{aligned} \quad (25)$$

The SK rate term is the experimental “thermometer” we use to remove most of the solar model “environmental” uncertainty, leaving in the next term SSM uncertainties that are dominated by the nuclear physics. But these uncertainties are, in some sense, under our control, and will be reduced as laboratory reaction measurements continue. The last terms are the primordial abundances we would like to constrain. The role of the SSM in this equation is to define a set of parameters and thus a set of reference rates, about which we then explore possible variations. Those variations generate the environmental and nuclear uncertainties given above, according to Eq. 11.

The R_{cal} factors in Eq. (25) contain additional uncertainties, including one important one:

- The shape of the normalized neutrino spectra: The ^{15}O shape spectrum is allowed, and thus accurately known. The ^8B spectrum is less certain because the β decay populates a broad

final-state resonance. In the SK analysis this spectrum error is among those included in the systematic error budget, so it should not be counted a second time. It contributes (Hosaka et al. 2006) at the $\sim 1\%$ level. This is a laboratory astrophysics uncertainty that could be lowered by improved measurements of the ^8Be resonance.

- Uncertainties in the elastic scattering cross section are also small ($\sim 0.5\%$ Hosaka et al. 2006), and furthermore tend to cancel between the two normalizing cross sections in Eq.(25).
- The principal uncertainty in the cross section ratio is that associated with neutrino oscillations. Apart from the dependence on the solar density profile, one can consider this to be another type of laboratory uncertainty: oscillation parameters can and will be further constrained by a variety of accelerator and reactor experiments. For example, KamLAND currently provides our best constraint on δm_{12}^2 .

The LMA parameter uncertainties in Super-Kamiokande and Borexino/SNO+ are anti-correlated. Most of the low-energy ^{15}N neutrinos do not experience a level crossing, residing instead in a portion of the MSW plane where the oscillations are close to the vacuum oscillation limit:

$$P_{\nu_e}(E_\nu) \rightarrow 1 - \frac{1}{2} \sin 2\theta_{12} \quad (26)$$

Thus an increase in the vacuum mixing angle θ_{12} decreases the ν_e survival probability. The higher energy ^8B neutrinos are largely within the MSW triangle, described by an adiabatic level crossing. The limiting behavior for an adiabatic crossing is

$$P_{\nu_e}(E_\nu) \rightarrow \frac{1}{2}(1 - \cos 2\theta_{12}) \quad (27)$$

so that an increase in θ_{12} increases the survival probability. This anti-correlation thus leads to larger effects in the ratio.

We have evaluated the impact of this uncertainty on Eq. (25), using the allowed regions for θ_{12} and δm_{12}^2 obtained in KamLAND’s combined analysis (Araki et al. 2005; The KamLAND Collaboration 2008), $0.833 \lesssim \sin^2 2\theta \lesssim 0.906$ and $7.38 \times 10^{-5} \text{ eV}^2 \lesssim \delta m_{12}^2 \lesssim 7.80 \times 10^{-5} \text{ eV}^2$. This yields

$$\frac{R_{cal}^{B/S}(^{15}\text{O}, \delta m_{12}^2, \theta_{12})}{R_{cal}^{SK}(^8\text{B}, \delta m_{12}^2, \theta_{12})^{0.825}} = (1 \pm 0.049) \left[\frac{R_{cal}^{B/S}(^{15}\text{O}, \delta m_{12}^2, \theta_{12})}{R_{cal}^{SK}(^8\text{B}, \delta m_{12}^2, \theta_{12})^{0.825}} \right]^{BV} \quad (28)$$

where BV denotes the best-value ratio.

Thus the overall uncertainty budget in Eq. 25 appears quite favorable, with the SK “thermometer” contributing at 3%, residual solar environmental uncertainties at 1%, and LMA parameter uncertainties at 4.9%. The largest of the errors is that from nuclear S-factor uncertainties,

currently 7.6%. The overall uncertainty in the “theoretical” relationship between a future SNO+ or Borexino CN-neutrino flux and core C/N metals is thus about 9.6%. As the nuclear physics uncertainty dominates the analysis, one would expect this relationship to become more precise when ongoing analyses of the full data set for $^{14}\text{N}(p,\gamma)$ are completed. An appropriate goal would be 3.5% in this S-factor, a 30% improvement. The uncertainty in $^{14}\text{N}(p,\gamma)$ would no longer dominate the nuclear physics error budget, but instead would be comparable to the contributions from S_{33} and S_{34} . However, the current 9.6% uncertainty is not a bad starting point, as first-generation CN-cycle neutrino experiments are expected to measure this flux to an accuracy of about 10%. That is, the theoretical uncertainty will not dominate the experimental uncertainty.

5. Future Experiments and Summary

One of the main motivations for this paper is the development of new detector ideas that might allow a high-statistics measurement of the CN-cycle neutrinos. In particular, detectors based on ultra-clean organic scintillation liquids have, at least in principle, the potential to make a high-sensitivity real-time measurement of the CN-cycle neutrinos.

The Borexino collaboration has investigated this possibility (The BOREXINO Collaboration 2005). Borexino, currently operating in Gran Sasso, has a 300-ton liquid scintillator target housed in a 8.5m spherical nylon membrane and shielded by a kiloton of buffer fluid. Events producing light within the detector are detected by an array of 2200 photomultiplier tubes. The inner 100 tons of the detector comprise the fiducial volume. The events come from elastic scattering off electrons, a reaction that is sensitive to both electron and (with reduced sensitivity) heavy-flavor neutrinos.

Borexino is primarily focused on detecting neutrinos from the pp chain, specifically the 862 keV line neutrinos from electron capture on ^7Be (the 90% branch). However, as mentioned previously, the collaboration has proposed using the detection window of (0.8-1.3) MeV to pick up contributions from the pep line source (1.442 MeV) and the ^{13}N and ^{15}O β decay sources.

The primary obstacle to such a measurement by Borexino is the *in situ* cosmogenic production of ^{11}C , a β^+ source. High-energy muons produced by primary cosmic ray interactions in the atmosphere can penetrate to great depths, producing ^{11}C by knocking a neutron out of ^{12}C . Borexino is located in Gran Sasso, which has a depth of about 3.1 kilometers of water equivalent (kmwe), when converted to the equivalent depth below a flat surface (Mei & Hime 2006). The ^{11}C production is still significant at this depth: an initial estimate of the associated background of 7.5 c/d/100 tons in Borexino was recently confirmed by a direct measurement (Back et al. 2006), yielding 13.0 ± 2.6 (stat) ± 1.4 (sys) c/d/100 tons. This exceeds the solar neutrino signal in the window of interest. Thus some means of vetoing this background must be introduced. This vetoing is nontrivial because of the long mean lifetime of ^{11}C , 29.4 minutes: a simple cut based on the muon would thus not be feasible.

The collaboration has proposed that a successful veto might be possible by exploiting a triple

coincidence, the initiating muon, the prompt capture of a neutron on protons in the scintillator fluid, and the delayed β^+ event (The BOREXINO Collaboration 2005; Deutsch, private communication). This would allow the experimenters to cut out a spherical volume defined by the neutron capture vertex, rejecting events within that volume for a time Δt large compared to the ^{11}C lifetime. The simulations performed by Borexino suggest that a signal/background ratio of 1.2 could be achieved with 20% deadtime. A CN-cycle neutrino (and pep neutrino) flux measurement could then be made by subtraction of this background.

An alternative to this approach would be to place such a detector at very great depth. This possibility has been discussed by the SNO+ collaboration, which has proposed placing a one-kiloton scintillator experiment in SNOLab, using the cavity that was originally excavated for SNO (Chen 2007). Such a detector could be used for detecting ^7Be , pep, and CN-cycle neutrinos, geoneutrinos, and double beta decay. The proposed volume is about a factor of three greater than that of Borexino. The great advantage of SNO+ would be its depth, 6.0 kmwe, and consequently its much lower cosmic ray muon background. The additional 3.0 kmwe, relative to Gran Sasso, provides about a factor of ~ 70 additional attenuation in the muon flux, so that the expected ^{11}C production would be reduced to ~ 0.1 c/d/100 tons, a few percent of the expected CN neutrino signal.

Figure 4 shows a simulation of the expected SNO+ response, performed by the experimenters (Chen, private communication). Note that the simulation is based on the BS05(OP) SSM and the best-fit LMA solution to the solar neutrino problem, rather than the updated BPS08(AGS) used in this paper. The CN-neutrino event rate for an energy window above 0.8 MeV was found to be 2300 counts/year. The experimenters concluded that SNO+ could determine the CN-neutrino rate to an accuracy of approximately 10%, after three years of running (Chen 2007). This accuracy is the appropriate goal for such a first-generation CN-cycle neutrino measurement, as it would approach the accuracy with which that flux could be related theoretically to the Sun’s primordial core C and N abundances, as we have argued in this paper.

In this paper we have suggested a possible strategy for using future Borexino/SNO+ CN-neutrino measurements as a test of the primordial C and N abundances in the solar core. The approach is based on using Super-Kamiokande as a solar thermometer, to largely eliminate other SSM uncertainties, so that a clean relationship between these abundances and CN neutrino rates can be made. SNO, KamLAND, and other neutrino oscillation experiments are used in the analysis to constrain LMA oscillation parameters. We derived a relationship where the dominant linear dependence on C and N remains, but other solar-model dependences are largely eliminated. This approach exploits the logarithmic derivatives that have been previously calculated for the SSM (especially those for the separate metal abundances) that define the impact of SSM parameter variations, supplemented by Monte Carlo calculations (which treat explicitly any correlations that may exist among the parameter variations). Although the relationship is derived in the context of the SSM, we suspect that it remains valid for a larger group of models, e.g., those where SSM parameters are varied well beyond their accepted SSM uncertainties: many investigators have shown that the ^8B neutrino flux remains a reliable thermometer, even when such large SSM parameter

variations are made.

We have found that the factors that limit the accuracy of Eq. (25) are first, uncertainties in nuclear cross sections ($\sim 7.6\%$) and second, uncertainties in LMA oscillation parameters ($\sim 4.9\%$). Both of these uncertainties can and will be reduced in future laboratory measurements. One goal should be the reduction, eventually, to the level of uncertainty of the SK thermometer, $\sim 3\%$.

In summary, it appears possible to use future experiments sensitive to CN-cycle neutrinos to constrain C and N content of the Sun’s primordial core. This would test an important assumption made in the SSM, that the zero-age Sun was homogeneous, with a core metallicity identical to that of today’s photosphere.

Such a measurement would also address a significant controversy, that recent 3D models of photospheric absorption lines have led to lower estimates of the abundances of the volatile metals. These new analyses appear to be on a solid foundation, substantially improving absorption line systematics and the consistency between the Sun and other similar stars in the local group. Yet they also significantly alter SSM predictions of the sound speed in the upper part of the Sun’s radiative zone, so that the SSM is no longer in good agreement with constraints imposed by helioseismology. For this reason, an independent measurement of the C and N abundances in the Sun’s radiative core would be of great interest.

This measurement would also place an important experimental constraint on the evolutionary history of the Sun. While the argument for a homogeneous Sun at the end of the pre-main-sequence Hayashi phase appears credible, once the Sun begins to form a radiative core, there are no subsequent SSM epochs that would allow mixing of the full Sun. Thus in principle any anomaly in the accretion of metals onto the Sun, either during the main sequence or in the Henyey phase, could produce chemical inhomogeneities. Such a scenario was the basis of the low-Z model, one of the proposed solar solutions to the puzzle posed by the chlorine experiment.

Unlike the low-Z model, a naive attempt to accommodate both the sound speeds required by helioseismology and the new photospheric abundances requires a convective zone depleted in metals. We have noted that the solar system’s primary reservoir for metals, the gaseous giant planets, are thought to have formed late relative to the evolution of the proto-Sun, incorporating an excess of metal estimated at $40\text{--}90 M_{\oplus}$. This mass is similar to the deficit of metals in the convective zone, were one to interpret the helioseismology/photospheric abundance discrepancy in the most naive way. This raises a provocative question: is it possible that the process that concentrated metals in the gaseous giants also produced a large volume of metal-depleted gas that subsequently was accreted onto the Sun’s surface? While the suggestion of a common chemical mechanism linking the convection zone and the gaseous giants is speculative, we think this is one more motivation for exploiting the CN neutrinos as a quantitative probe of solar core metallicity.

We thank M. Chen, P. Goldreich, K. Snover, Y. Suzuki, and M. Wiescher for discussions. This work was supported in part by the Office of Nuclear Physics, US Department of Energy, under

grant DE-FG02-00ER-41132. AMS is supported by the IAS through a John Bahcall Fellowship and NSF grant PHY-0503584.

REFERENCES

- Abdurashitov, J. N., et al. 2003, Nuclear Physics B Proceedings Supplements, 118, 39
- Adelberger, E. G., et al. 1998, Reviews of Modern Physics, 70, 1265
- Aharmim, B., et al. 2005, Phys. Rev. C, 72, 055502
- Ahmad, Q. R., et al. 2001, Physical Review Letters, 87, 071301
- Ahmad, Q. R., et al. 2002, Physical Review Letters, 89, 011301
- Ahmad, Q. R., et al. 2002, Physical Review Letters, 89, 011302
- Antia, H. M. & Basu, S. 2005, ApJ, 620, L129
- Araki, T., et al. 2005, Physical Review Letters, 94, 081801
- Arpesella, C., et al. 2008, Physics Letters B, 658, 101
- Asplund, M., Grevesse, N., & Sauval, A. J. 2005, in Astronomical Society of the Pacific Conference Series, Vol. 336, Cosmic Abundances as Records of Stellar Evolution and Nucleosynthesis, ed. T. G. Barnes, III & F. N. Bash, 25
- Back, H., et al. 2006, Phys. Rev. C, 74, 045805
- Badnell, N. R., Bautista, M. A., Butler, K., Delahaye, F., Mendoza, C., Palmeri, P., Zeippen, C. J., & Seaton, M. J. 2005, MNRAS, 360, 458
- Bahcall, J. N. 1989, Neutrino astrophysics (Cambridge and New York, Cambridge University Press, 1989, 584 p.)
- Bahcall, J. N., Basu, S., Pinsonneault, M., & Serenelli, A. M. 2005a, ApJ, 618, 1049
- Bahcall, J. N. & Davis, R. 1976, Science, 191, 264
- Bahcall, J. N. & Pinsonneault, M. H. 2004, Physical Review Letters, 92, 121301
- Bahcall, J. N., Pinsonneault, M. H., & Basu, S. 2001, ApJ, 555, 990
- Bahcall, J. N. & Serenelli, A. M. 2005, ApJ, 626, 530
- Bahcall, J. N., Serenelli, A. M., & Basu, S. 2005b, ApJ, 621, L85
- Bahcall, J. N., Serenelli, A. M., & Basu, S. 2006, ApJS, 165, 400

- Bahcall, J. N. & Ulrich, R. K. 1988, *Reviews of Modern Physics*, 60, 297
- Bemmerer, D., et al. 2006, *Nuclear Physics A*, 779, 297
- Bodenheimer, P. & Lin, D. N. C. 2002, *Annual Review of Earth and Planetary Sciences*, 30, 113
- Brown, T. A. D., Bordeanu, C., Snover, K. A., Storm, D. W., Melconian, D., Sallaska, A. L., Sjue, S. K. L., & Triambak, S. 2007, *Phys. Rev. C*, 76, 055801
- Brun, A. S., Turck-Chièze, S., & Morel, P. 1998, *ApJ*, 506, 913
- Brun, A. S., Turck-Chièze, S., & Zahn, J. P. 1999, *ApJ*, 525, 1032
- Castellani, V., degl’innocenti, S., Fiorentini, G., Lissia, M., & Ricci, B. 1994, *Phys. Rev. D*, 50, 4749
- Castro, M., Vauclair, S., & Richard, O. 2007, *A&A*, 463, 755
- Chen, M. C. 2007, in *American Institute of Physics Conference Series*, Vol. 944, American Institute of Physics Conference Series, 25–30
- Confortola, F., et al. 2007, *Phys. Rev. C*, 75, 065803
- Csótó, A. & Langanke, K. 2000, *Few-Body Systems*, 29, 121
- Davis, R., Harmer, D. S., & Hoffman, K. C. 1968, *Physical Review Letters*, 20, 1205
- Descouvemont, P., Adahchour, A., Angulo, C., Coc, A., & Vangioni-Flam, E. 2004, *Atomic Data and Nuclear Data Tables*, 88, 203
- Fiorentini, G. & Ricci, B. 2003, *ArXiv Astrophysics e-prints*
- Formicola, A., et al. 2004, *Physics Letters B*, 591, 61
- Fukuda, S., et al. 2001, *Physical Review Letters*, 86, 5651
- Fukuda, S., et al. 2002, *Physics Letters B*, 539, 179
- Fukuda, Y., et al. 1996, *Physical Review Letters*, 77, 1683
- Grevesse, N. & Sauval, A. J. 1998, *Space Science Reviews*, 85, 161
- Guillot, T. 2005, *Annual Review of Earth and Planetary Sciences*, 33, 493
- Gyürky, G., et al. 2007, *Phys. Rev. C*, 75, 035805
- Hosaka, J., et al. 2006, *Phys. Rev. D*, 73, 112001
- Imbriani, G., et al. 2005, *European Physical Journal A*, 25, 455

- Kajino, T. & Arima, A. 1984, *Physical Review Letters*, 52, 739
- Kirsten, T. A. 2003, *Nuclear Physics B Proceedings Supplements*, 118, 33
- Lemut, A., et al. 2006, *Physics Letters B*, 634, 483
- Mei, D.-M. & Hime, A. 2006, *Phys. Rev. D*, 73, 053004
- Mohapatra, R. N., et al. 2004, *ArXiv High Energy Physics - Phenomenology e-prints*, arXiv:hep-ph/0412099
- Montalbán, J., Miglio, A., Noels, A., Grevesse, N., & di Mauro, M. P. 2004, in *ESA Special Publication*, Vol. 559, *SOHO 14 Helio- and Asteroseismology: Towards a Golden Future*, ed. D. Danesy, 574–+
- Nara Singh, B. S., Hass, M., Nir-El, Y., & Haquin, G. 2004, *Physical Review Letters*, 93, 262503
- Peña-Garay, C. & Serenelli, A. M. 2008, in preparation
- Podolak, M., Hubbard, W. B., & Pollack, J. B. 1993, in *Protostars and Planets III*, ed. E. H. Levy & J. I. Lunine, 1109–1147
- Runkle, R. C., Champagne, A. E., Angulo, C., Fox, C., Iliadis, C., Longland, R., & Pollanen, J. 2005, *Physical Review Letters*, 94, 082503
- Saumon, D. & Guillot, T. 2004, *ApJ*, 609, 1170
- Strom, S. E., Edwards, S., & Skrutskie, M. F. 1993, in *Protostars and Planets III*, ed. E. H. Levy & J. I. Lunine, 837–866
- The BOREXINO Collaboration. 2005, *Nuclear Physics B Proceedings Supplements*, 145, 29
- The KamLAND Collaboration. 2008, *ArXiv e-prints*, 801
- Trautvetter, H. P., et al. 2008, *Journal of Physics G Nuclear Physics*, 35, 4019
- Winnick, R. A., Demarque, P., Basu, S., & Guenther, D. B. 2002, *ApJ*, 576, 1075
- Wuchterl, G. & Klessen, R. S. 2001, *ApJ*, 560, L185

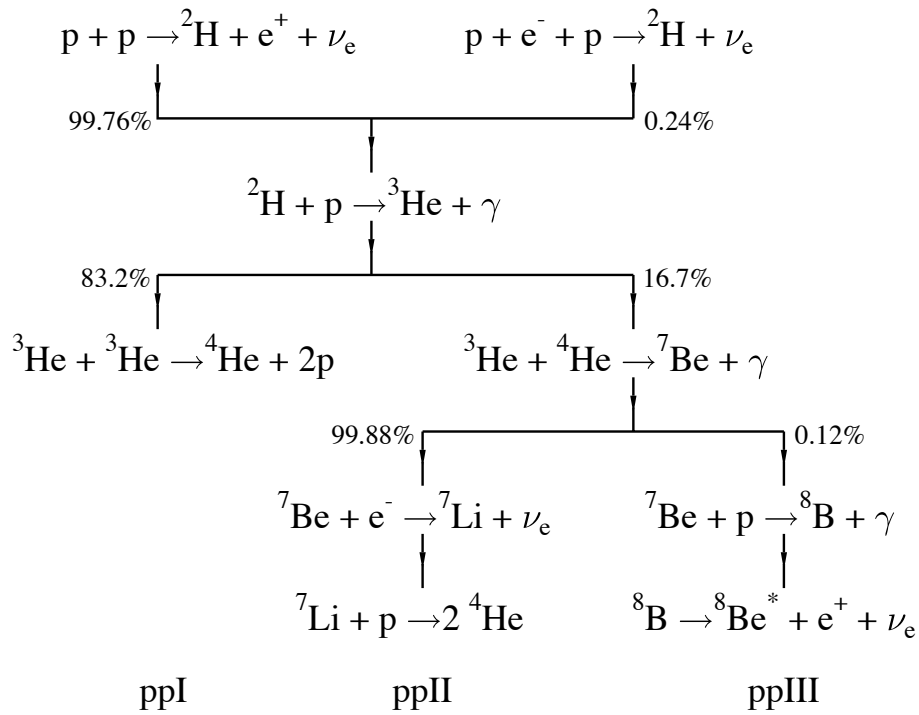


Fig. 1.— The pp-chain for hydrogen burning. The relative termination rates of competing reactions correspond to the BPS08(AGS) SSM.

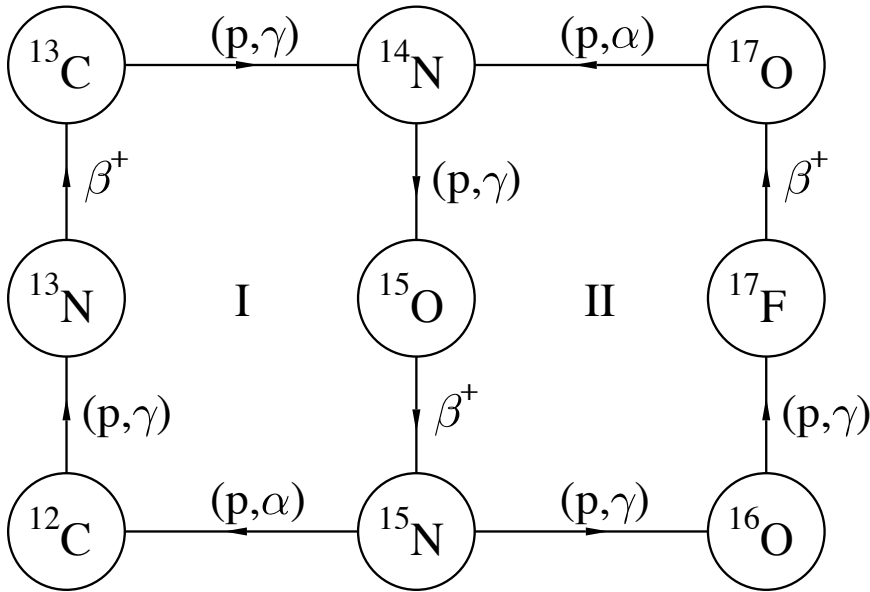
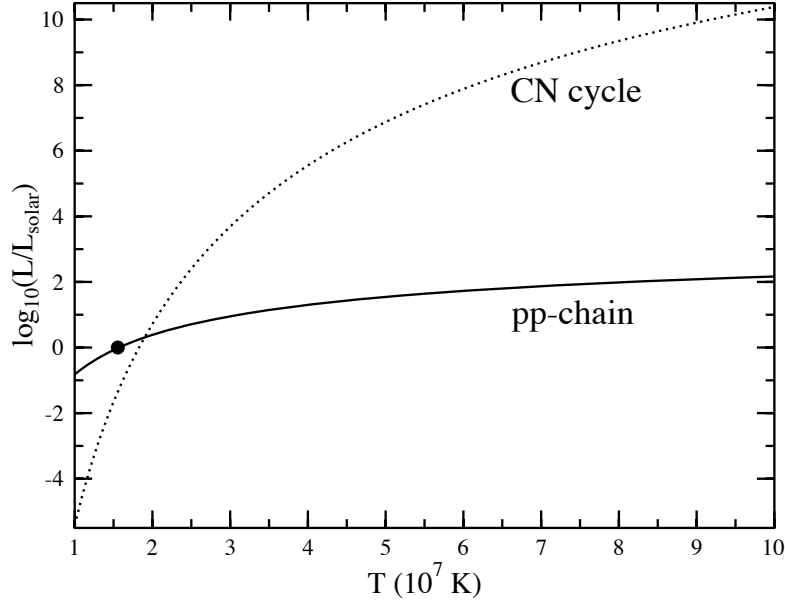


Fig. 2.— The lower panel shows the CNO bi-cycle for hydrogen burning. The upper panel compares the energy produced in the CN cycle with that produced in the pp-chain, as a function of temperature T_7 , measured in units of 10^7 K. The results are normalized to the pp-chain energy production in the Sun’s central core and to solar metallicity, and assume the burning is in equilibrium. The sharp CN-cycle dependence on temperature is apparent. If approximated as a power law T^x , x ranges between ~ 19 and ~ 22 over the range of temperatures typical of the Sun’s hydrogen-burning core. The dot marks the point corresponding to the Sun’s center, $T_7 = 1.57$.

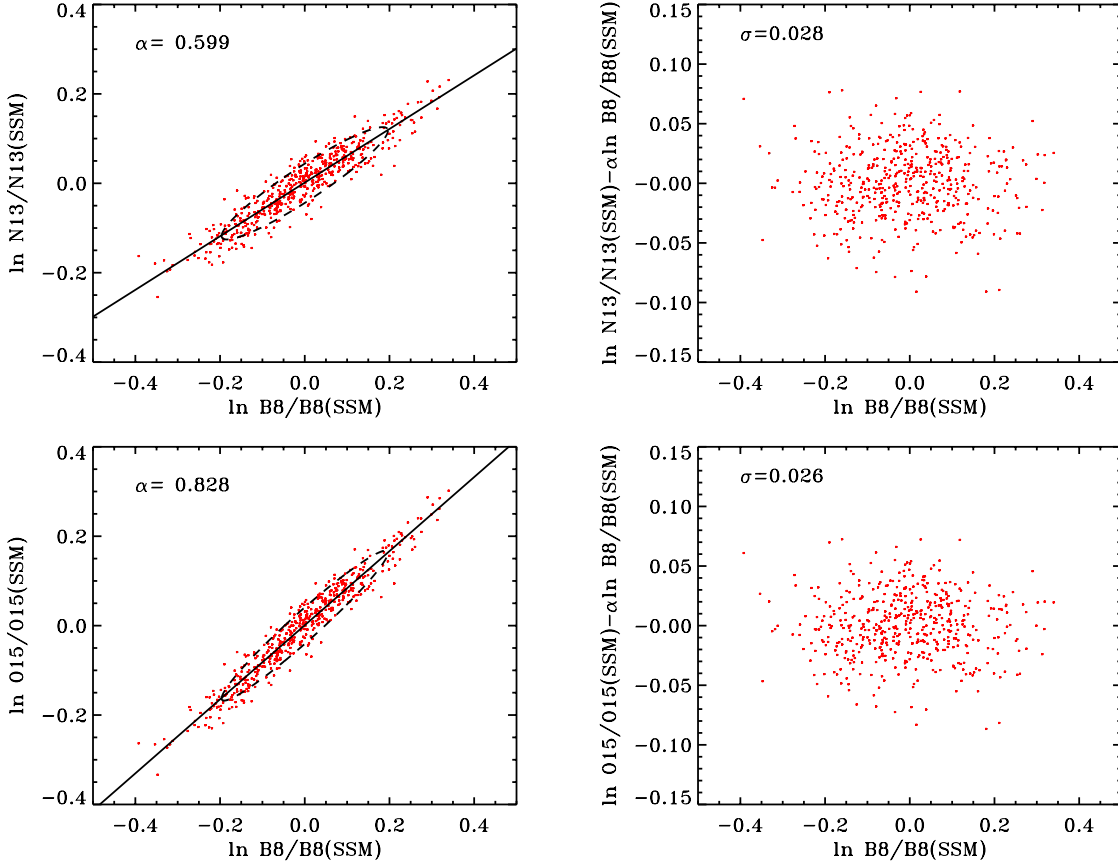


Fig. 3.— Results from a Monte Carlo simulation of SSM where the 11 environmental parameters (see text) have been varied. The two left panels show the correlations between the ^8B flux and the two CN-cycle neutrino fluxes ^{13}N and ^{15}O . The slopes of the correlations are given in the plots, together with the 68.3% confidence level contours. On the right side panels we show the residuals from the fits, 2.8% and 2.6% for the ^{13}N and ^{15}O fluxes respectively, that determine the residual environmental uncertainty in Eqs. (9,13) respectively.

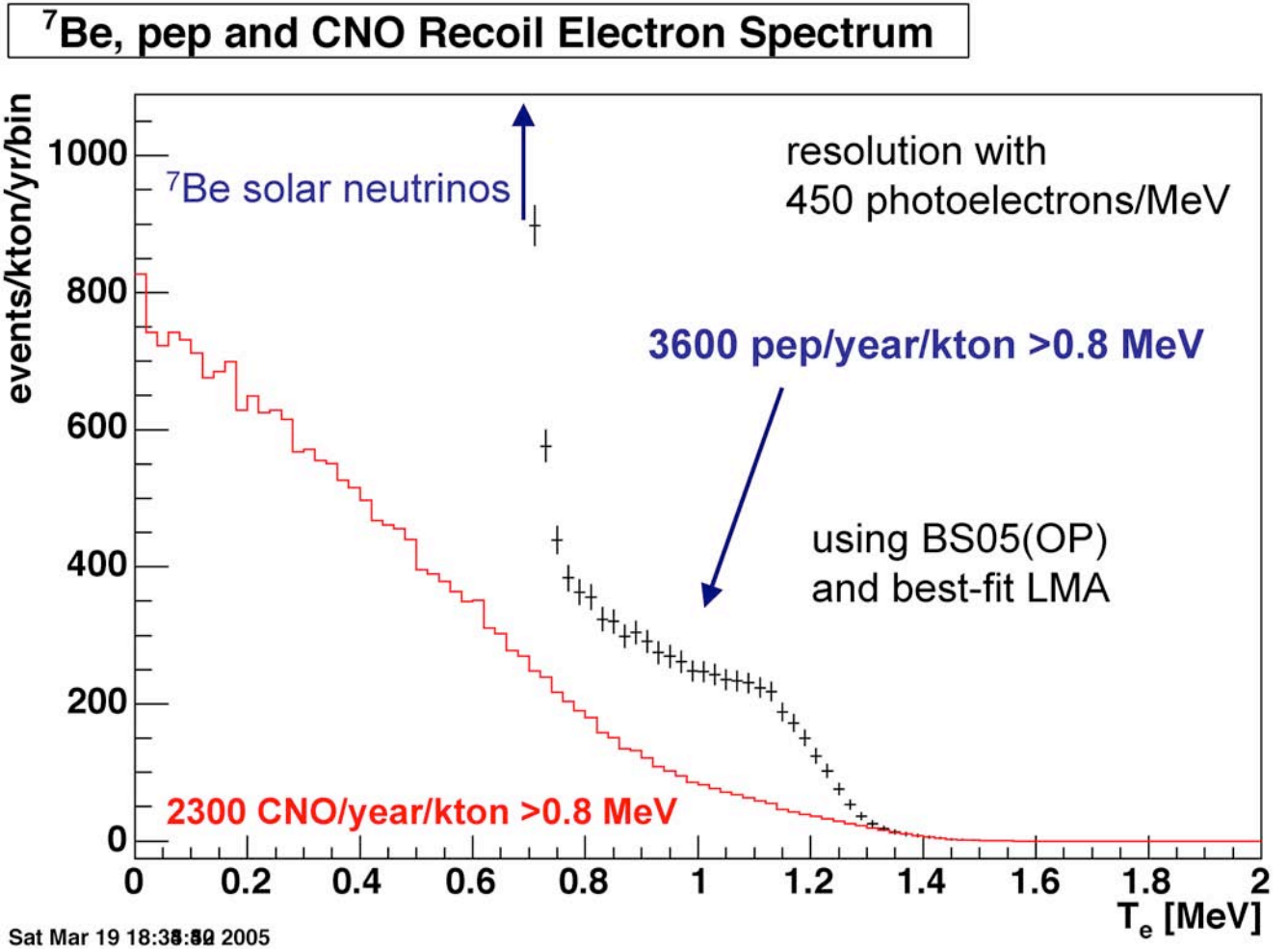


Fig. 4.— A simulation of events expected in SNO+, the proposed SNOLab experiment to measure low-energy solar and other neutrino sources. This figure is due to M. C. Chen (Chen 2007).

Table 1. Partial derivatives $\alpha(i, j)$ of neutrino fluxes with respect to solar environmental and nuclear cross section parameters.

Source	Environmental β_j				Nuclear β_j					
	L_\odot	Opacity	Age	Diffusion	S_{11}	S_{33}	S_{34}	S_{17}	S_{e7}	S_{114}
$\phi(^8\text{B})$	7.16	2.70	1.38	0.28	-2.73	-0.43	0.85	1.0	-1.0	-0.020
$\phi(^{13}\text{N})$	4.40	1.43	0.86	0.34	-2.09	0.025	-0.053	0.0	0.0	0.71
$\phi(^{13}\text{N})/\phi(^8\text{B})^{0.599}$	0.11	-0.19	0.03	0.17	-0.45	0.28	-0.56	-0.60	0.60	0.72
$\phi(^{15}\text{O})$	6.00	2.06	1.34	0.39	-2.95	0.018	-0.041	0.0	0.0	1.00
$\phi(^{15}\text{O})/\phi(^8\text{B})^{0.828}$	0.07	-0.18	0.20	0.16	-0.69	0.37	-0.74	-0.83	0.83	1.02

Note. — Table entries are the logarithmic partial derivatives $\alpha(i, j)$ of the solar neutrino fluxes ϕ_i with respect to the indicated solar model parameter β_j , taken about the SSM best values. All fluxes are in units of their SSM best values, and thus are dimensionless. The derivatives, taken from Peña-Garay & Serenelli (2008), are for the SSM BPS08(AGS), which employs the AGS abundances. The two flux ratios were determined for a $\phi(^8\text{B})$ exponent that minimizes the residual environmental error in the prediction, including the environmental variables here and in Table 2. As explained in the text, that error is weighted according to the uncertainties in the environmental parameters β_j , given in Table 3.

Table 2. Partial derivatives $\alpha(i, j)$ of neutrino fluxes with respect to fractional abundances of the primordial heavy elements.

Source	C, N β_j		Environment Abundance β_j						
	C	N	O	Ne	Mg	Si	S	Ar	Fe
$\phi(^8\text{B})$	0.027	0.001	0.107	0.071	0.112	0.210	0.145	0.017	0.520
$\phi(^{13}\text{N})$	0.874	0.142	0.044	0.030	0.054	0.110	0.080	0.010	0.268
$\phi(^{13}\text{N})/\phi(^8\text{B})^{0.599}$	0.858	0.141	-0.020	-0.013	-0.013	-0.016	-0.007	0.000	-0.043
$\phi(^{15}\text{O})$	0.827	0.200	0.071	0.047	0.080	0.158	0.113	0.013	0.393
$\phi(^{15}\text{O})/\phi(^8\text{B})^{0.828}$	0.805	0.199	-0.018	-0.012	-0.013	-0.016	-0.007	-0.001	-0.038

Note. — Heavy elements are divided into “environmental” metals – those which primarily influence the solar core through their effects on the opacity and thus the core temperature – and C and N, which govern the production of ^{13}N and ^{15}O solar neutrinos and which can be determined, in principle, from measurements of these fluxes. Results correspond to the BPS08(AGS) model (Peña-Garay & Serenelli 2008).

Table 3. Estimated 1σ uncertainties in solar and nuclear SSM parameters, taken from Bahcall, Serenelli, and Basu Bahcall et al. (2006) and Fiorentini and Ricci Fiorentini & Ricci (2003), and their influence on flux predictions, computed from the partial derivatives of Table 1. The experimental value for S_{17} is taken from a series of recent measurements: this S -factor and S_{114} are discussed in the text.

β_j	Value	$\Delta\beta_j/\beta_j(\%)$	$\Delta\phi(^8\text{B})/\phi(^8\text{B})(\%)$	$\Delta\phi(^{13}\text{N})/\phi(^{13}\text{N})(\%)$	$\Delta\phi(^{15}\text{O})/\phi(^{15}\text{O})(\%)$
L_\odot	3.842×10^{33} ergs/s	0.4	2.9	1.8	2.4
Opacity	1.0	2.5	6.9	3.6	5.2
Age	4.57 b.y.	0.44	0.61	0.38	0.59
Diffusion	1.0	15.0	4.0	4.9	5.7
p+p	3.94×10^{-25} MeV b	0.4	1.1	0.84	1.2
$^3\text{He}+^3\text{He}$	5.4 MeV b	6.0	2.5	0.15	0.10
$^3\text{He}+^4\text{He}$	0.564 MeV b	4.9	4.1	0.25	0.20
p+ ^7Be	20.6 eV b	3.8	3.8	0.0	0.0
e+ ^7Be		2.0	2.0	0.0	0.0
p+ ^{14}N	1.61 keV b	5.0	0.1	3.5	5.0

Table 4. Estimated 1σ historical (“conservative”) uncertainties in AGS abundances, as defined in Bahcall & Serenelli (2005). The corresponding uncertainties in the neutrino fluxes are computed from the partial derivatives of Table 2.

β_j	$\Delta\beta_j/\beta_j(\%)$	$\Delta\phi(^8\text{B})/\phi(^8\text{B})(\%)$	$\Delta\phi(^{13}\text{N})/\phi(^{13}\text{N})(\%)$	$\Delta\phi(^{15}\text{O})/\phi(^{15}\text{O})(\%)$
C	29.7	0.70	25.5	24.0
N	32.0	0.03	4.0	5.7
O	38.7	3.6	1.4	2.3
Ne	53.9	3.1	1.3	2.0
Mg	11.5	1.2	0.59	0.87
Si	11.5	2.3	1.2	1.7
S	9.2	1.3	0.71	1.0
Ar	49.6	0.69	0.40	0.53
Fe	11.5	5.8	3.0	4.4